Effect of Wall-surrounded Slot on Stepped Narrow-wall for Bandwidth Enhancement of Partially-parallel Feeding Waveguide Travelling-wave Array

Yuichi Hirayama, Kunio Sakakibara, *Senior Member, IEEE*, Haruki Umemura, Katsuhiro Miyazaki, and Nobuyoshi Kikuma, *Senior Member, IEEE*

***Abstract*—A partially-parallel feeding system of travelling-wave waveguide slot array has an advantage to reduce the frequency dependence of excitation phase of slots cut on the waveguide, which results in broadband feature of gain and radiation pattern. However, a conventional narrowband post-loaded radiating slot for array element limits the overall bandwidth of the array. A broadband wall-surrounded slot on a stepped narrow-wall in the waveguide is proposed in this work. The effects of the step on the waveguide narrow-wall and the walls surrounding slot are evaluated individually by electromagnetic simulation in this paper. The proposed antenna configuration of the waveguide assembled at the waveguide center allows to fabricate by plastic molding with metal plating. The antenna performance is measured to confirm the feasibility of the proposed antenna in the millimeter-wave band.**

***Index Terms*—Antenna arrays, Antenna feeds, Broadband antennas, Millimeter wave antenna arrays, Slot arrays, Waveguide**

I. Introduction

MILLIMETER-WAVE technologies have already been widely applied to automotive radar systems [1], [2]. A high-speed millimeter-wave WiFi in WiGig (IEEE802.11ad) technologies is going to be practical in the market very soon [3], [4]. The fifth generation mobile communication (5G) systems are hot topics in millimeter-wave research and development toward service in 2020 [5], [6]. Next generation automotive UWB radars are assigned over 77-81GHz to achieve high range resolution, which is wider than 4 times of the current automotive radars. The high-capacity millimeter-wave communication systems also require wide frequency bandwidth in general.

Slotted waveguide arrays are attractive for low-loss property, therefore, suitable for high-gain applications. We have developed a high-gain two-dimensional array with travelling-wave operation [7]. The narrow-wall slot on the waveguide allows us assembling the two metal plates with waveguide grooves separated at the center of the broad walls. The transmission loss is still low, because the high-frequency current flows in the parallel direction to the gap between the two metal plates, even though the physically small gap can not be ignored in the millimeter-wave band. Consequently, narrow-wall slots can be an advantageous slot configuration of the slotted waveguide arrays in the millimeter-wave band.

The array-feeding configuration affects to the structural complexity, bandwidth, and feeding loss significantly. A series feeding array of travelling-wave excitation is composed of the array elements sequentially connected to the feeding line, which results in a geometrically-simple feeding structure of an array in general [8]. However, in this case, the element spacing is determined as one guided wavelength for in-phase excitation, which reflects to the frequency dependence of the beam direction and limits the bandwidth. On the other hand, a parallel feeding system is a tournament configuration as a combination of two-way power-dividers [9]. The design is simple and no frequency dependence exists in the array configuration. However, the length of the feeding line is electrically long, which causes significant transmission loss in the design of a large array. In the case of waveguide feeding, as transmission loss is low, the feeding loss is not significant. However, the structure of the feeding waveguide is quite complicated for the parallel feeding. Therefore, partially-parallel feeding waveguide systems have been proposed for the balance between broadband with high gain and structure simplicity.

A partially-cooperate feeding two-dimensional broad-wall slotted waveguide array with high gain in broad bandwidth has been developed [10]. High gain of 33dBi over broad bandwidth was achieved. However, forming a waveguide without gaps on the walls, a diffusion bonding technique was applied in fabrication of simple double layered waveguide structure. We have developed a partially-parallel feeding slotted waveguide array [11], [12]. A vertically long array with 12 x 2 elements was composed for a sub-array of digital beam forming (DBF)

This work was supported by JSPS KAKENHI Grant Number JP 15H04005.

The authors are with the Department of Electrical and Mechanical Engineering, Nagoya Institute of Technology at Nagoya, Aichi, 466-8555 Japan (e-mail: sakaki@nitech.ac.jp).

systems to detect the direction of arrival in horizontal plane. High efficiency was obtained by assembling the narrow-wall slotted waveguide at the center of the broad wall, even though only two metal grooves are screwed. The partially-parallel feeding system was broadband, however, the operation bandwidth of the radiating elements composed of a slot with a post in the waveguide and a circular wall on the outside were narrow. Consequently, the overall bandwidth of the array was limited. To solve this issue, a broadband wall-surrounded radiating slot on a stepped narrow-wall of a waveguide was proposed [13]. The slot spacing for in-phase excitation is one guided wavelength, which is longer than a wavelength in free space. To prevent generating grating lobes, an interleave arrangement with a half guided wavelength shift of adjacent linear arrays on the narrow-width narrow-walls are applied by using a four-way power divider for feeding in 180-degrees opposite phase. The effects of the surrounding wall and the step for bandwidth extension were investigated individually by electromagnetic simulation of finite element method in this paper.

Various waveguide forming techniques have been developed for low-cost manufacturing. A substrate integrated waveguide (SIW) can be formed in a substrate as well as a microstrip line [14], [15]. Via holes are arranged to work for narrow wall of the waveguide. Thick substrate is necessary to reduce conductor loss. A diffusion bonding technique of a number of patterned metal plates is a possible way to manufacture two-dimensional waveguide arrays [9], [10], [16]. The material of the metal is limited to heavy metals such as copper, nickel, or iron. 3D printing technique is becoming popular and applied to antenna fabrication [17], [18]. Accurate fabrication of antennas for millimeter-wave band is still difficult and time consuming, therefore, low cost and mass production are still difficult. However, fabrication of arbitrary structures is possible. Electro-forming technique is also demonstrated for antenna fabrication [19]. Plastic molding with metal plating has been applied for antenna manufacturing [20], [21]. It is attractive at the accurate 3D forming, arbitrary structure by molding, light weight of plastic, and low cost due to mass production.

The feasibility of the proposed antenna was evaluated in 80GHz band by experiments of the waveguide array fabricated by plastic molding with metal plating in this work. The simple and low loss configuration of the waveguide assembled at the broad-wall center of the waveguide slotted on the narrow wall allows us to fabricate the antenna by plastic molding with metal plating. The antenna configuration was indicated in Sec. II. The design was explained in Sec. III. The performance of the proposed antenna was demonstrated by simulations and measurements in Sec. IV. Finally, this paper was summarized by conclusion in Sec. V.

II. Antenna Configuration

A. Partially-parallel Feeding Travelling-wave Array

A vertically long planar array with radiating slots 12 x 2 was designed for sub-arrays of digital beam forming systems in the millimeter-wave band. A partially-parallel feeding system is composed of double-layer waveguide circuit as shown in Fig. 1. The feeding waveguide in the lower layer is fed from the side via waveguide E-plane T-junction. The both ends of the feeding waveguide are terminated by E-plane H-plane composite bends. To realize Taylor distribution on the aperture for sidelobe level lower than −20dB, an asymmetrical four-way power divider with three-element travelling-wave waveguide arrays was designed. The four-way power divider is fed from each composite bend and provides different power to the inner and the outer three-element travelling-wave arrays.

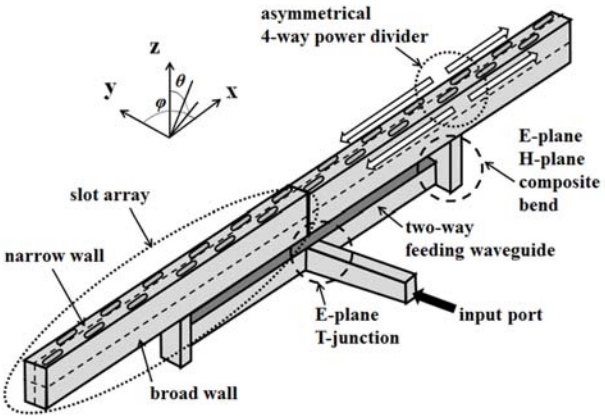

Fig.1 Partially-parallel feeding travelling-wave waveguide slot array composed of feeding circuit of E-plane T-junction and E-plane H-plane composite bends in lower layer and asymmetrical 4-way power dividers and three-element travelling slot arrays in upper layer.

The slots are arranged on the radiating waveguide with spacing of one guided wavelength for in-phase excitation. To prevent generating grating lobes, the broad-wall width was designed to be larger for shorter guided wavelength and the adjacent waveguides are fed with 180 degrees phase difference out of phase for triangular lattice slot arrangement. The narrow-wall width was designed to be small to avoid generating grating lobes in the diagonal planes. Consequently, the spacing between the sub-arrays of digital beam-forming systems can be small for large beam-scan angle. Thus, a 24-element slotted waveguide array was obtained. The designs of the radiating slot and the feeding circuit are explained in the following sections.

B. Wall-surrounded Slot on Stepped Waveguide Narrow-wall

To take advantage of the broad bandwidth of the parallel-feeding configuration of the array, a broadband radiating element was proposed. The structure of the element is shown in Fig. 2. The radiating slot is cut on the narrow wall of the waveguide in parallel to the waveguide axis. The two plates with upper and lower grooves are assembled to compose the radiating waveguide at the center of the broad wall where the electric current flows in parallel with the waveguide axis and is not cut by the assembled plane.

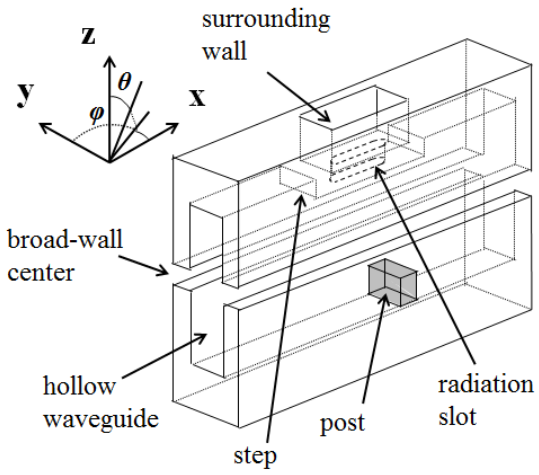

Fig. 2 Wall-surrounded slot on stepped narrow-wall of the radiating waveguide with post on the opposed narrow-wall.

A post is loaded by a radiating slot for matching to cancel their reflections out of phase in the conventional antennas [7]. As mentioned in Sec. II A, the broad-wall width was designed to be larger for shorter guided wavelength. Consequently, the power density in the waveguide around the slot becomes lower. The post works to concentrate the transmitting power around the slot, which increases the coupling power to the air from the slot. However, the appropriate height of the post is higher than a half of the broad-wall width when the coupling power to the air is designed to be large for slots arranged near the termination of the travelling-wave array. The exceeding height of the post over the depth of the lower groove causes difficulty of manufacturing.

To increase the coupling power from the slot, even though the height of the post is low, a step is located on the narrow wall of the radiating waveguide and the slot is cut on the step. Thus, the slot on the step approaches to the post in the waveguide. Large coupling is obtained even though the height of the post is low. The power density in the waveguide around the slot becomes strong without exceeding the height of the post over the depth of the lower groove. Furthermore, three reflections from a step, a slot, and a post are canceled out each other. As each of the three reflections is lower than each of the two reflections from the slot and the post without the step in the conventional radiating element, therefore, broadband characteristics are expected. As a slot is surrounded by a rectangular wall outside of the waveguide, the cavity structure increases the electrical size of the resonant structure, which reduces Q factor and contributes to extend the bandwidth.

C. Feeding Circuit of Partially-Parallel Feeding System

To enhance the bandwidth of the entire array, the partially-parallel feeding system was introduced [9]. The feeding system of the antenna is composed of a two-way feeding waveguide fed by the E-plane T-junction and two asymmetrical four-way power dividers. The structure of the two-way feeding waveguide is shown in Fig. 3. A post is located at the corners

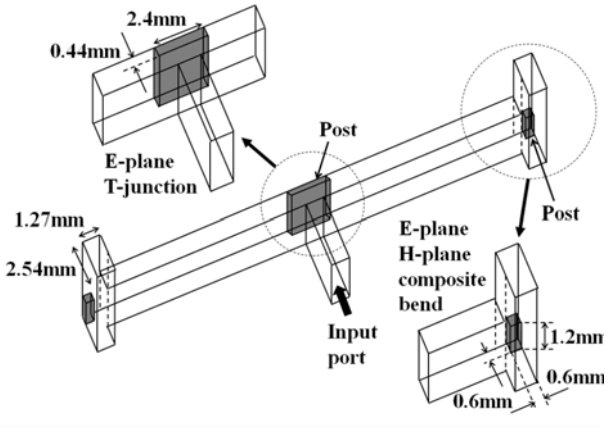

Fig. 3 Center feeding waveguide circuit in the lower layer composed of E-plane T-junction and E-plane H-plane composite bends at the both ends of the feeding waveguide.

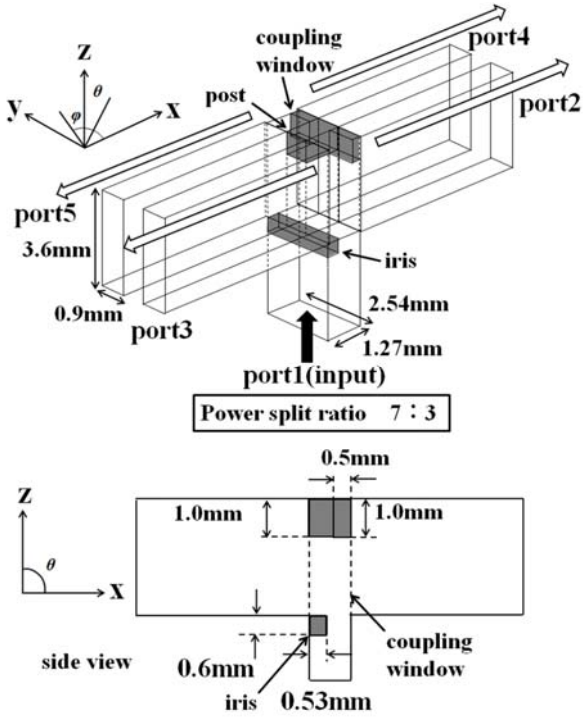

Fig. 4 Four-way power divider with asymmetrical dividing ratio feeding four three-element travelling slot arrays.

of the E-plane T-junction and the E-plane H-plane composite bends. The size of the post is optimized for impedance matching by electromagnetic simulation. The asymmetrical four-way power divider is shown in Fig. 4. To realize Taylor distribution on the aperture for sidelobe level lower than −20dB, an asymmetrical four-way power divider with power dividing ratio 7:3 to inner and outer three-element travelling-wave arrays. The iris and the coupling window are installed to adjust the power dividing ratio 7:3. A post is located at the opposite side of the input port for impedance matching.

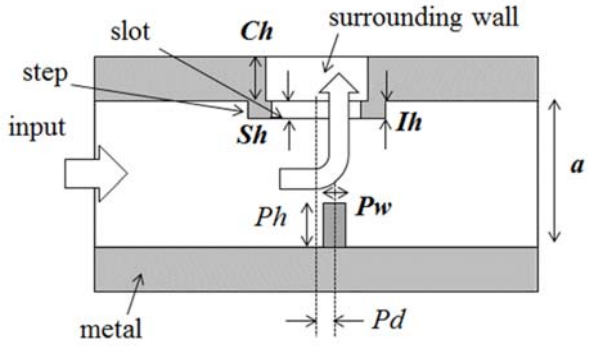

(a) cross-sectional side view

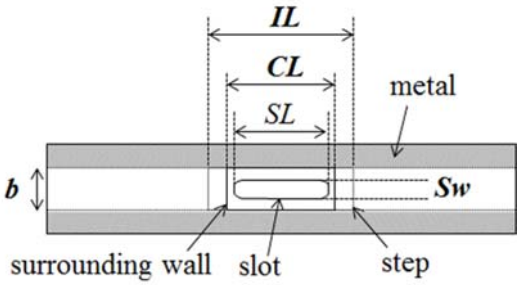

(b) top view

Fig. 5 Side and top views in the waveguide and geometrical parameters of wall-surrounded slot on stepped narrow-wall.

TABLE I
DIMENSIONS OF WALL-SURROUNDED SLOT ON STEPPED NARROW-WALL

geometry (variable)	dimension [mm]
broad-wall width (*a*)	3.3
narrow-wall width (*b*)	0.9
slot height (*Sh*)	0.4
slot width (*Sw*)	0.4
post width (*Pw*)	0.5
height of surrounding wall (*Ch*)	1.0
length of surrounding wall (*CL*)	2.3
height of step (*Ih*)	0.4
length of step (*IL*)	3.1

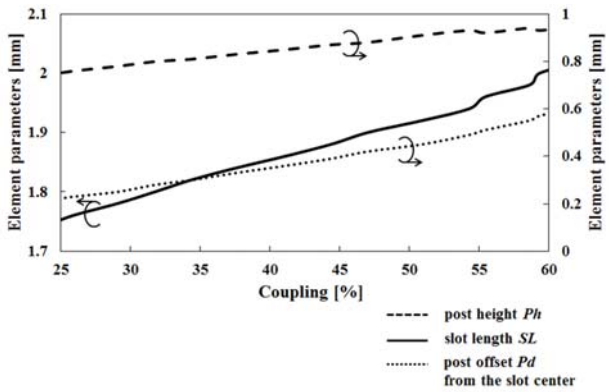

Fig. 6 Variations of the slot dimensions (post height *Ph*, slot length *SL*, post offset *Pd* from the slot center) depending on the coupling power to the air from the slot.

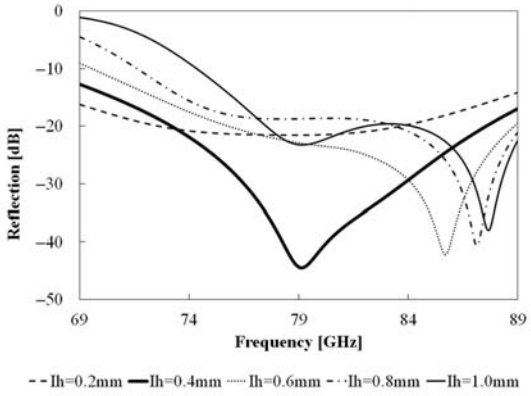

Fig. 7 Frequency characteristics of reflection for the wall-surrounded slot on the stepped narrow-wall depending on the height *Ih* of the step on the narrow wall.

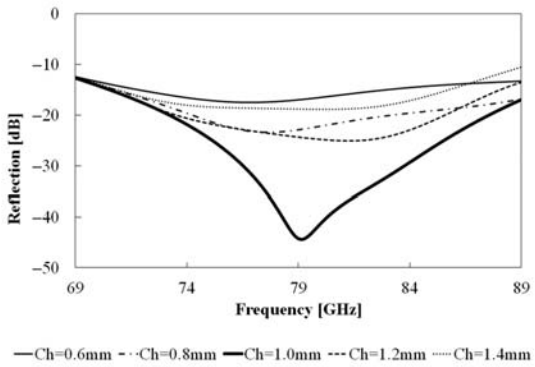

Fig. 8 Frequency characteristics of reflection for the wall-surrounded slot on the stepped narrow-wall depending on the height *Ch* of the step on the narrow wall.

III. DESIGN

A. Design of Wall-surrounded Slot on Stepped Waveguide Narrow-wall

The geometrical parameters of a wall-surrounded slot on a stepped narrow-wall of the radiating waveguide are defined in Fig. 5. The designed dimensions are listed in Table I. The broad-wall width *a* is determined to be larger for shorter guided wavelength at the upper limit the higher order TE_{20} mode does not generate. The narrow-wall width *b* is determined to be small to avoid generating grating lobes in diagonal plane of the triangular arrangement of the array and to reduce the spacing of adjacent sub-arrays in DBF systems. The narrow-wall width *b* and the slot height *Sh*, the slot width *Sw*, and the post width *Pw* are determined by the limitation for manufacturing plastic molding with metal plating. The geometrical parameters of the slot length *SL*, the post height *Ph*, and the post offset *Pd* from the slot center related to the coupling power are shown in Fig. 6. The coupling power is controlled by the slot length *SL*. A tall post is necessary to cancel large reflection from a long slot. The phase of reflection wave from the post is controlled by the offset *Pd* from the slot center to cancel the reflection from the slot out of phase. Figure 7 shows the frequency characteristics of the reflection for the wall-surrounded slot on the stepped narrow-

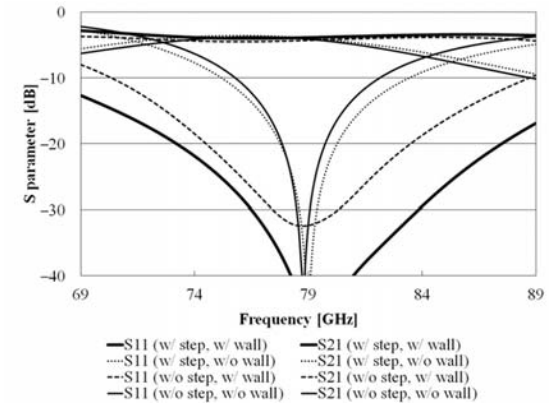

Fig. 9 Frequency dependency of S_{11} and S_{21} of array elements when the coupling is 60%.

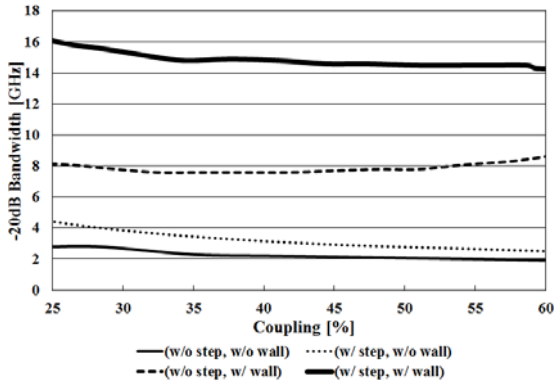

Fig. 10 Variation of coupling dependency for bandwidths of reflection lower than −20dB of the radiating elements with/without surrounding wall and with/without step to show the effect of surrounding wall and step for bandwidth enhancement.

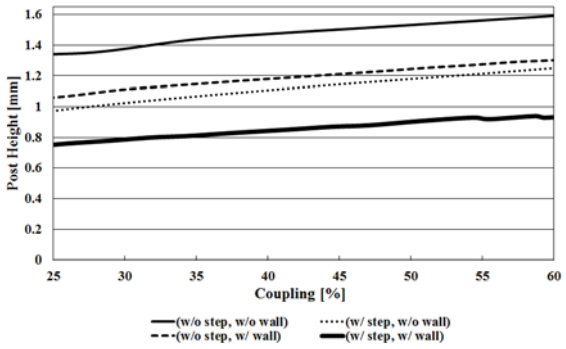

Fig. 11 Variation of coupling dependency for post height *Ph* of the radiating elements with/without surrounding wall and with/without step to show the effect of surrounding wall and step to reduce post height.

wall depending on the height *Ih* of the step. When the height *Ih* of the step is low, the reflection does not drop. However, when the height *Ih* of the step grows higher, the reflection drops and the resonant frequency shifts higher due to the cut off feature reducing the broad-wall width. When *Ih* was 0.4mm, the resonant frequency was identical to the design frequency 79GHz. Consequently, broad bandwidth was obtained. The reflection dropped at the design frequency 79GHz when the

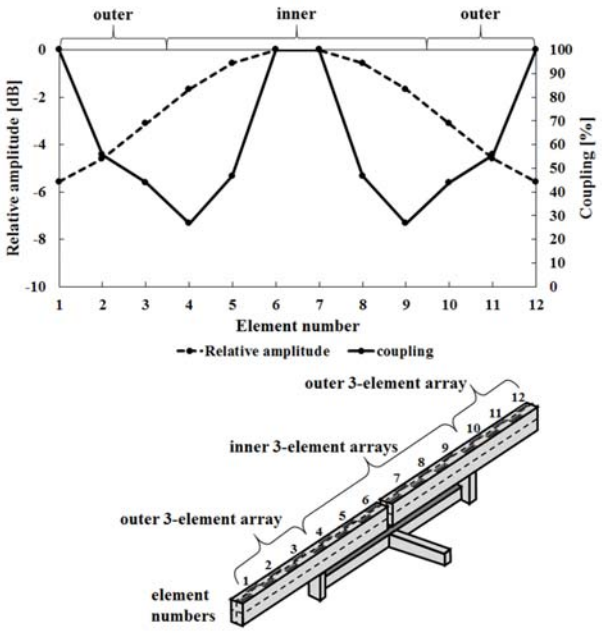

Fig. 12 Taylor distribution and required coupling on the aperture for sidelobe level lower than −20dB.

height *Ch* of the surrounding wall was 1.0mm which is approximately a quarter wavelength, as is shown in Fig. 8.

The reflection characteristics of the radiating element were simulated to confirm the effect of the step on the narrow wall and the surrounding wall individually. The bandwidths for reflection lower than −20dB were compared in the same coupling power. When the coupling power is 60%, the step extends the bandwidth by 1.32 times and the surrounding wall does by 4.53 times as shown in Fig. 9. The effects of the bandwidth extension for coupling variation are summarized for whole coupling power in Fig. 10. When the coupling is 25%, the step extends the bandwidth by 1.57 times and the surrounding wall does by 2.89 times. When both a step and a wall are used, the bandwidths are extended by 7.53 times for 60% coupling and by 5.75 times for 25%. It is confirmed that the effect of the step is not large independently for bandwidth extension, however, the step amplifies the effect of the wall for broad bandwidth drastically. The Post height for coupling variation was compared in Fig. 11. The step lowers the post height by 0.37mm on average and the wall does by 0.29 mm on average. When both a step and a wall are used, the post height is lower by 0.62 mm on average. The effect of the proposed structure for lower post height was also confirmed.

B. Array Design

The slot length *SL*, the post height *Ph*, and the post offset *Pd* from the slot center are variables and were designed to obtain low reflection characteristic for each required coupling in Taylor distribution on the aperture. The Taylor distribution for sidelobe level lower than −20dB and the required coupling values on the aperture are shown in Fig. 12. The asymmetrical power divider in a dividing power ratio of 7:3 to inner and outer

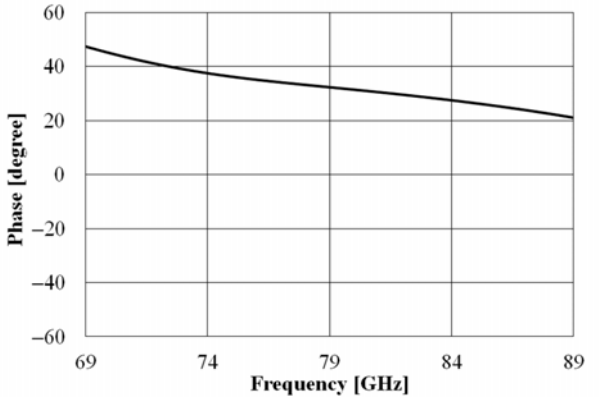

Fig. 13 Perturbation of transmission phase S_{21} of element No. 4.

TABLE II ELEMENT SPACING IN ONE RADIATING WAVEGUIDE. (ELEMENT NUMBERS ARE DEFINED IN FIG. 12.)

Element Number	1-2	2-3	3-4	4-5	5-6	6-7	7-8	8-9	9-10	10-11	11-12
Element Spacing	5.71	4.81	6.50	4.88	5.49	4.47	5.49	4.88	6.50	4.81	5.71

three-element short-ended travelling-wave arrays was used as mentioned in Sec. II C. The coupling power of radiating slots from 26% to 56% is necessary for travelling-wave array. The termination slot with a short circuit is designed to radiate all input power.

The element spacing is designed to realize uniform aperture phase distribution for broadside beam in the traveling-wave design. Essentially, the slots are excited in-phase when the spacing is one guided wavelength. However, the guided wavelength depends on the broad-wall width of the rectangular waveguide. The guided wavelength is partly longer at the stepped narrow-wall. The element spacing is determined to be longer taking the phase perturbation due to the step and the slot into account. The perturbation of the transmission phase of the element No. 4 is shown in Fig. 13. The transmission phase was perturbed by 32degrees at the design frequency 79GHz. The phase perturbation was taken into account in the array design. The designed element spacing is listed in Table II. The guided wavelength is 4.64mm at 79GHz when the broad wall width a is 3.3mm. The phase perturbation increases for larger coupling to termination. Therefore, the element spacings between the elements numbered 1 and 2, 5 and 6, 7 and 8, 11 and 12 are much larger than the guided wavelength. Furthermore, the element spacing between 3 and 4, 9 and 10 are much larger, where the four-way power dividers are located under these spaces. This slot arrangement reflects to radiation patterns of the array. The simulated and measured radiation patterns will be evaluated in the next section IV.

C. Design of Feeding Circuit

The reflection characteristic of the two-way feeding waveguide composed of the center T-junction and two E-plane H-plane composite bends at the both ends of the feeding waveguide shown in Fig. 3 was simulated and is shown in Fig. 14. Although the characteristic depends on the distance between the E-plane T-junction and the E-plane H-plane composite bends, the bandwidth for reflection lower than −20dB was 8.8GHz. The reflection characteristic and the power dividing ratio of the asymmetrical 4-way power divider shown in Fig. 4 are shown in Fig. 15. The bandwidth of reflection lower than −20dB was 3.1GHz. The power split ratio was 72.7% and 27.3% for inner and outer three-element travelling-wave arrays, respectively.

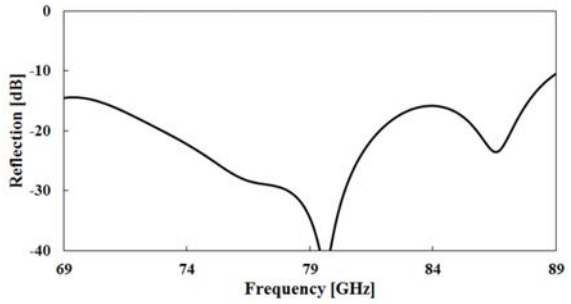

Fig. 14 Reflection characteristic of the feeding circuit in the lower layer composed of an E-plane T-junction and two E-plane H-plane composite bends shown in Fig. 3.

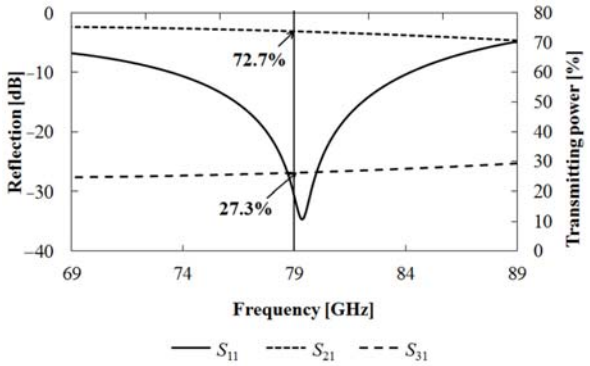

Fig. 15 Reflection characteristic and power dividing ratio of an asymmetrical 4-way power divider shown in Fig. 4.

IV. Simulated and Measured Performances

The proposed antenna was designed and the feasibility was confirmed by simulations and measurements. The design frequency was 79GHz. The developed antenna was compared with the conventional antenna whose radiating elements were composed of only a slot and a post. The design frequency was 76.5GHz and the broad-wall width a was 3.6mm, while that of the developed antenna was 3.3mm, as listed in TABLE I.

The fabricated antenna was composed of four copper-plated plastic plates as shown in Fig. 16(a). The base plastic plates were fabricated by precision cutting. Therefore, the accuracy depends on the cutting process as well as cutting solid metal. Thickness of the copper was approximately 10μm on the whole plastic surface with nickel thinner than 0.1μm for corrosion resistant coating. The theoretical skin depth of copper is

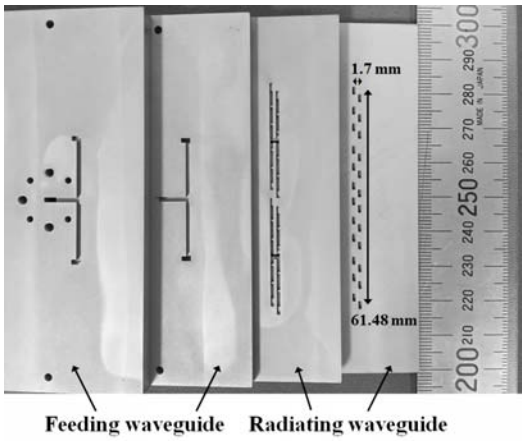

(a) The fabricated antenna composed of four plastic plates with metal plating. The radiating and feeding waveguides are assembled by two plates for each.

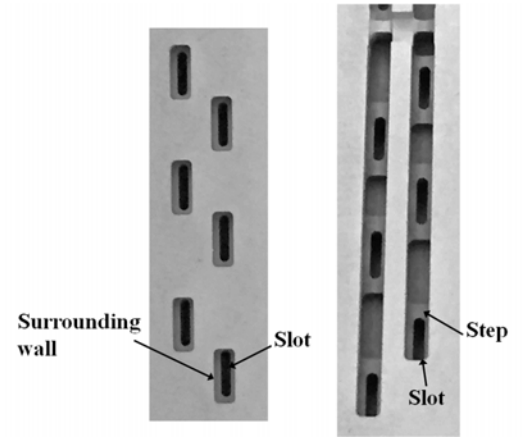

(b) Top view (left) to show the wall-surrounded slot and inner view (right) to show the stepped narrow-wall.

Fig. 16 The photograph of the fabricated antenna using plated plastic technology.

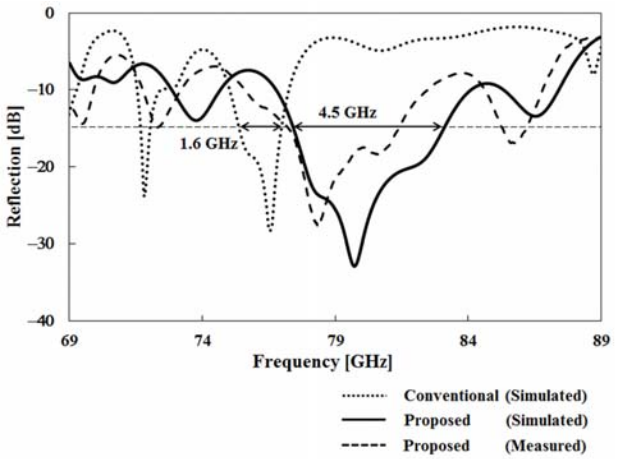

Fig. 17 Simulated and measured reflection characteristics of the proposed antenna comparing the simulated characteristic of the conventional antenna.

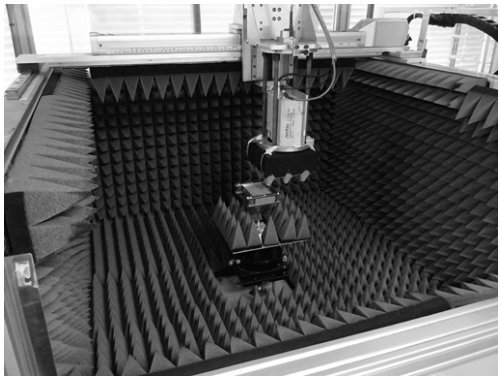

Fig. 18 Near-field measurement system with XY scanner.

0.23μm. The thickness of the plated copper is much thicker than the skin depth. Therefore, the conductivity is equivalent with the fabrication from a solid cupper. Both the feeding and the radiating waveguides were assembled by two grooves at the center of the waveguide broad-wall and the two waveguides were connected together. The feeding waveguide was assembled by attaching the upper planes of the left two pieces in Fig. 16(a) whose reflection characteristics were evaluated in Sec. III C as is shown in Fig. 14. The radiating waveguide was assembled by attaching the upper plane of the second right piece and the lower plane of the first right piece, which includes two center-feeding slot arrays fed from two four-way power dividers evaluated in Fig. 15. The four plates are assembled only by screws. The array length was 61.5mm and the spacing between the center axises of the two radiating waveguides was 1.7mm. The narrow-wall steps extend into the radiating waveguides and the slot was cut on each step as shown in Fig. 16(b). The surrounding wall was formed at the outside of the waveguide on each slot.

The bandwidth of simulated reflection lower than −15dB, which corresponds to 3% reflection loss, was 5.6GHz which is 3.5 times of 1.6GHz of the conventional one as shown in Fig. 17. The bandwidth of measured reflection lower than −15dB was 4.5GHz. The measured resonant frequency shifted by 1.3GHz lower than the simulated one. This may be caused by 1.6% error of antenna dimensions in the fabrication. However, the bandwidth of the measured reflection lower than -15dB still covers 4.1GHz because of the wideband characteristic.

Radiation patterns were obtained by Fourier transformation of the XY near-field measurement data. The photograph of the measurement system is shown in Fig. 18. The port 1 of the vector network analyzer Anritsu ME7808 is connected to the AUT set on the stage at the center of the chamber. The port 2 of the VNA is connected to the probe scanning over the AUT. Accurate measurement can be performed, however, large angle far from the broadside direction is not accurate due to only using two dimensional near-field XY data. The simulated and measured radiation patterns of co-polarization and cross-polarizations are shown in Fig. 19. The cross-polarization is not radiated from all parallel slots essentially. Therefore, measured cross-polarization level is almost lower than −30dB. To investigate the influence of the designed non-uniform slot

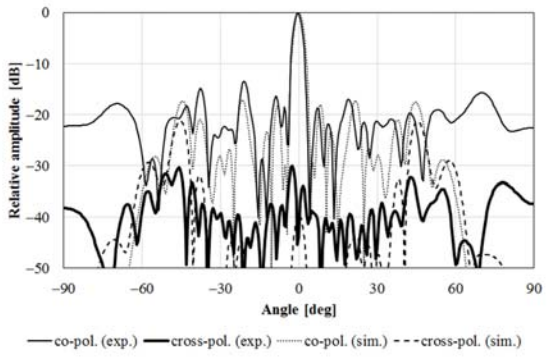

Fig. 19 Simulated and measured radiation patterns of co- and cross-polarizations at 79GHz.

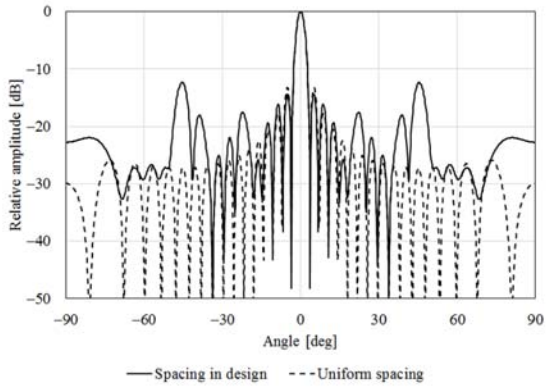

Fig. 20 Array factors of the arrays whose slot spacings are designed and uniform.

arrangement to radiation patterns, the array factor of uniform amplitude and phase aperture distributions in the same slot arrangement with the design whose slot spacing is listed in Table II is compared with the array factor of the uniform slot spacing in Fig. 20. The first sidelobe level is 1.1dB lower rather than the uniform slot spacing. However, sidelobes at 22.2, 39.0, and 45.2 degree directions are higher than the uniform slot arrangement due to the non-uniformity of the designed slot arrangement. Therefore, the higher sidelobes were observed around 20, 40, 45 degree directions in Fig. 19. However, the first sidelobe level was limited to −15dB by the effect of the Taylor distribution in the design.

Figure 21 shows the frequency dependency of the antenna gain. The simulated peak gain was 20.7dBi and the bandwidth 14.6GHz of gain higher than 15dBi was almost twice of the conventional one. The bandwidth of the measured gain higher than 15dBi was 12.5GHz. The measured peak gain was 19.8dBi which is 0.9dB lower than simulation. Significant loss was not observed in the experiments. The simulated gain increases at first rapidly then slowly with frequency from 74GHz until a cutoff around 85GHz. This behavior is from the aperture theory combined with the operating bandwidth of the antenna. However, the measured gain drop starts at 79GHz. This is considered together with the strong increase of the reflection shown in Fig. 17 and the transmission loss of the plated plastic waveguide. The shift of the operation frequency observed in Fig. 17 could be also one of the reasons. The effect of the reflection

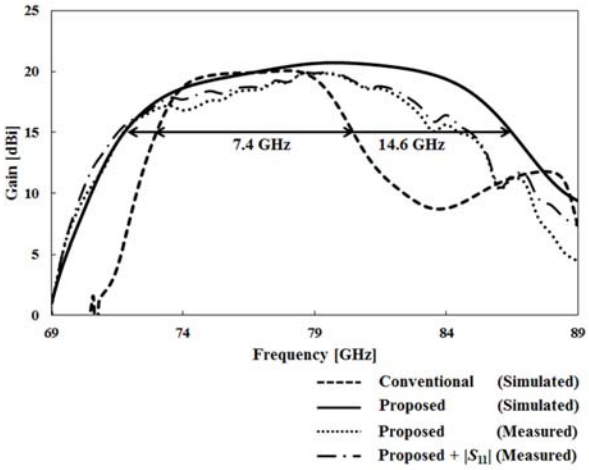

Fig. 21 Frequency dependency of the antenna gain.

increase for the gain drop was approximately 0.8dB maximum at 83.5GHz observed as a difference from the measured gain excluding the return loss. Figures 22 shows the radiation pattern variation depending on the frequency. The beam direction was stable for frequency change due to the symmetrical structure. However, the directivity dropped due to the phase tapers in the opposite inclination between the both halves on the aperture in the 6GHz frequency shift. Consequently, the effects of proposed radiating element and the feeding circuit were observed in the performance of the entire array.

V. Conclusion

The wall-surrounded slot on the stepped narrow-wall of the waveguide was proposed to extend the bandwidth of the radiating elements. A 24-element two-line partially-parallel feeding waveguide slot array antenna was designed in the millimeter-wave band. The bandwidth of reflection lower than −20dB for the proposed radiating element was over 7GHz, then, the bandwidth of reflection lower than −15dB which corresponds to 3% reflection loss for the entire array was extended by 3.5 times to 5.6GHz in contrast to 1.6GHz bandwidth of the conventional post-loaded slot. The gain of the broadside direction was higher than 15dBi in 72.0-86.6GHz and peak gain was 20.7dBi. The bandwidth of the measured reflection lower than −15dB was 4.5GHz and that of the gain higher than 15dBi was 12.5GHz. Consequently, the wide bandwidth of the reflection and the gain of the entire array were obtained and the effect of the proposed structure was confirmed. The narrow-wall slotted waveguide configuration assembled at the broad-wall center allows to fabricate the antenna composed of four plated-plastic plates screwed together.

References

[1] J. Hasch, “Driving towards 2020: Automotive radar technology trends,” 2015 IEEE MTT-S International Conference on Microwaves for Intelligent Mobility (ICMIM), April 27-29, 2015

[2] H. H. Meinel and J. Dickmann, “Automotive Radar: From Its Origins to Future Directions,” Microwave Journal, Sep., 2013.

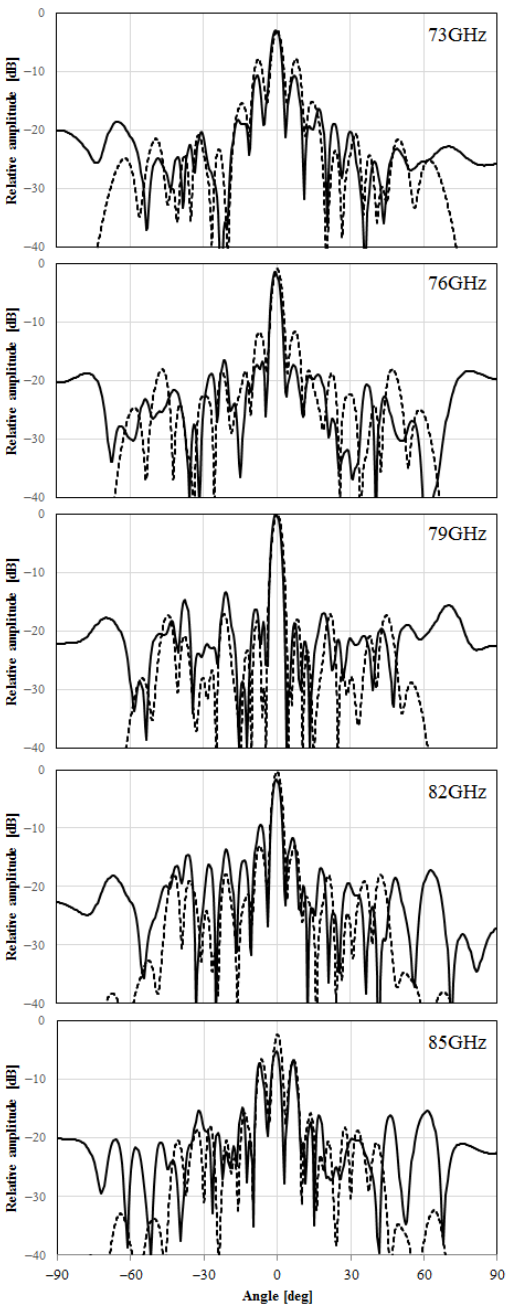

Fig. 22 Radiation pattern variation depending on frequency normalized by the peak at 79GHz (solid line: measured, dotted line: simulated).

[3] C. J. Hansen, "WiGiG: Multi-gigabit wireless communications in the 60 GHz band," IEEE Wireless Communications, Vol.18, Issue.6, pp.6-7, Dec. 2011.

[4] " Qualcomm 802.11ad Products to Lead the Way for Multi-band Wi-Fi Ecosystem," Qualcomm Press Release, Las Vegas, Jan. 2016.

[5] T. S. Rappaport, W. Roh and K. Cheun, "Smart Antennas Could Open Up New Spectrum For 5G," IEEE SPECTRUM, Aug 2014.

[6] K. Sakaguchi, G. K. Tran, H. Shimodaira, S. Nanba, T. Sakurai, K. Takinami, I. Siaud, E. C. Strainati, A. Capone I. Karls, R. Arefi and T. Haustein, "Millimeter-Wave Evolution for 5G Cellular Networks," IEICE Trans. on Commun., Vol.E98-B, No.3, pp.388-402, March 2015.

[7] A. Mizutani, K. Sakakibara, N. Kikuma, H. Hirayama, "Grating Lobe Suppression of Narrow-Wall Slotted Hollow Waveguide Millimeter-Wave Planar Antenna for Arbitrarily Linear Polarization," IEEE Trans. on Antennas Propagation, Vol. 55, No. 2, pp. 313-320, Feb. 2007.

[8] J. L. Volakis, Antenna Engineering Handbook, Fourth Edition, Chap. 9, Mc Graw Hill, 2007

[9] T. Tomura, J. Hirokawa, T. Hirano, and M. Ando, "A Wideband 16 x 16-Element Corporate-Feed Hollow-Waveguide Slot Array Antenna in the 60-GHz Band," vol. E97-B, No. 4, pp. 798-806, April 2014.

[10] M. Zhang, J. Hirokawa, M. Ando, "A Partially-Corporate Feed Double-Layer Waveguide Slot Array with the Sub-Arrays also Fed in Alternating-Phases," IEICE Trans. on Commun., vol. E97-B, No. 2, pp. 469-475, Feb. 2014.

[11] Y. Ikeno, K. Sakakibara, N. Kikuma, H. Hirayama, " Narrow-Wall-Slotted Hollow-Waveguide Array Antenna Using Partially Parallel Feeding System in Millimeter-Wave Band, " IEICE Transactions on Communications, Vol.E93-B No.10 pp.2545-2553, October 2010.

[12] A. Kunita, K. Sakakibara, N. Kikuma, and H. Hirayama, "Broadband Millimeter-Wave Microstrip Comb-Line Antenna Using Corporate Feeding System with Center-Connecting," IEICE Trans. on Communications, Vol. E95-B, No. 1, pp. 41-50, Jan. 2012

[13] K. Sakakibara, Y. Hirayama, K. Miyazaki, K. Shiotani, Y. Miyachi, and N. Kikuma, "Bandwidth Enhancement of Partially Parallel-feeding Travelling-wave Array using Waveguide Narrow-wall Cavity Slot on Iris in Millimeter-wave Band," 2016 IEEE International Symposium on Antennas and Propagation and CNC-USNC/URSI Radio Science Meeting Digest, Puerto Rico, June, 2016.

[14] Y. J. Cheng, W. Hong, T. Djerafi and K. Wu, "Substrate-Integrated-Waveguide Beamforming Networks and Multibeam Antenna Arrays for Low-cost Satellite and Mobile Systems," IEEE Antennas Propag. Magazine, vol.53, No.6, pp.18-30, Dec.2011.

[15] K. Hashimoto, J. Hirokawa, and M. Ando, "A Post-Wall Waveguide Center-Feed Parallel Plate Slot Array Antenna in the Millimeter-Wave Band," IEEE Trans. on Antennas Propag., vol. 58, No. 11, pp. 3532-3538, Nov. 2010.

[16] Y. Miura, J. Hirokawa, M. Ando, Y. Shibuya, and G. Yoshida, "Double-Layer Full-Corporate-Feed Hollow-Waveguide Slot Array Antenna in the 60-GHz Band," IEEE Trans. on Antennas Propag., vol. 59, No. 8, pp. 2844-2851, Aug. 2011.

[17] J. S. Chieh, B. Dick, S. Loui, and J. D. Rockway, "Development of a Ku-Band Corrugated Conical Horn Using 3-D Print Technology," IEEE Antennas and Wireless Propag. Letters, vol. 13, pp. 201-204, 2014.

[18] G. P. Le Sage, "3D Printed Waveguide Slot Array Antennas," IEEE Access, vol. 4, pp. 1258-1265, March 21, 2016.

[19] D. Kim, Y. Lim, H. Yoon, and S. Nam, "High-Efficiency W-Band Electroforming Slot Array Antenna," IEEE Trans. on Antennas and Propag., vol. 63, No. 4, pp. 1854-1857, April 2015.

[20] E. G. Geterud, P. Bergmark, J. Yang, "Lightweight Waveguide and Antenna Components Using Plating on Plastics," 2013 7th European Conference on Antennas and Propagation (EuCAP), pp. 1812-1815, Gothenburg, Sweden, April 8-12, 2013.

[21] Y. Konishi, T. Nishino, H. Yukawa, and Y. Aramaki, "Millimeter-wave plastic waveguide phased array antenna," 2010 IEEE Antennas and Propag. Society Interntl. Symp., pp. 1-4, Toronto, Canada, July 11-17, 2010.